Probing the hot-electron transport properties and interface band structure of Fe/Si (001) and $Fe_{81}C_{19}$/Si (001) Schottky diodes

A. J. Stollenwerk, M. R. Krause, D. H. Idell, R. Moore, and V. P. LaBella
College of Nanoscale Science & Engineering, University at Albany-SUNY, Albany New York 12203, USA
(Received 2 June 2006; revised manuscript received 25 August 2006; published 27 October 2006)

Ballistic electron emission microscopy (BEEM) has been performed on both Au/$Fe_{81}C_{19}$/Si (001) and Au/Fe/Si (001) Schottky diodes at 80 K. The Schottky heights were measured to be 0.68±0.02 eV and 0.70±0.02 eV for the $Fe_{81}C_{19}$/Si (001) and Fe/Si (001) interfaces, respectively. In addition, a second threshold voltage was observed for the Fe/Si (001) interface at 1.29±0.04 eV and attributed to an additional conduction band minimum at the interface that arises from the bonding of the Fe to the Si. The hot electron attenuation lengths at 1.25 eV were measured to be 3.5±1.0 nm and 3.0±0.9 nm for $Fe_{81}C_{19}$ and Fe, respectively. The attenuation length of the $Fe_{81}C_{19}$ showed a decrease with increasing energy consistent with the universal curve for electron-electron scattering. However, the attenuation length for the Fe showed this decrease only until the onset of the second threshold after which it increased. It is proposed that this increase is attributed to the parallel momentum distribution of the additional conduction band minimum at the Fe/Si (001) interface.

DOI: 10.1103/PhysRevB.74.155328 PACS number(s): 73.40.−c

I. INTRODUCTION

Ferromagnetic thin-film Schottky contacts have been utilized for spin injection into semiconductors.[1] Studying the transport and interface properties of these structures can provide a fundamental understanding of the mechanisms that influence electron transport and injection. One method for studying ballistic electron transport through thin metal films, metal-metal interfaces, and metal-semiconductor interfaces is ballistic electron emission microscopy (BEEM).[2,3] This three-terminal scanning tunneling microscopy (STM) technique injects electrons from a STM tip into a grounded metal base of a Schottky diode. A small fraction of these electrons will travel ballistically through the metal to the metal-semiconductor interface where they will encounter a Schottky barrier. Those electrons with sufficient energy to surmount the Schottky barrier will be detected by a backside contact as BEEM current (I_{BEEM}). The atomic-scale positioning capability of the STM tip gives BEEM nanometer spatial resolution.[4] In addition, the narrow energy distribution of electrons tunneling from the STM tip gives BEEM a high energetic resolution (~0.02 eV).[3–5]

Transition metal/silicon and transition metal silicide/silicon interfaces have rich physical characteristics which have been illuminated using BEEM. The most notable is $CoSi_2$, where atomic-scale BEEM images have been obtained.[5] In addition, different values for the Schottky height have been recorded that have not been sufficiently explained.[3,6] Theoretical first-principles calculations of the $NiSi_2$/Si (001) interface predict differences in BEEM spectra due to a change in the interface structure but have not been observed in experimental BEEM studies possibly due to scattering in the silicide.[7–9] In addition, BEEM spectra for MnSi/Si (001) displayed multiple thresholds that arose from an additional conduction band minimum (CBM) at the interface.[10] Thickness-dependent BEEM studies of Fe, Co, Ni, and $Ni_{81}Fe_{19}$ on Si (001) at room temperature have yielded Schottky heights that range from 0.65 eV to 0.90 eV depending on the type of metal and its thickness.[11] In addition, an attenuation length of 0.5 nm at 1.5 eV for Fe thicknesses in the range of 0.2–2.0 nm has been reported.[12] Some recent BEEM studies have been performed on $Fe_{81}C_{19}$-silicon Schottky diodes that measured a Schottky height of 0.70 eV and hot electron attenuation length of 2.5 nm at 1.5 eV, different from the previous study for pure Fe.[12,13] However, no attempt to compare the effect of carbon, a common additive in Fe, on the ballistic electron transport properties in Fe has been reported to date.

In this article, the Schottky height and ballistic electron attenuation length of Fe and $Fe_{81}C_{19}$ are measured at 80 K using BEEM. A second threshold was observed in the Fe films due to the existence of a second conduction band minimum at the interface. In addition, the attenuation lengths decrease with increasing tip bias, consistent with electron-electron scattering. However, the attenuation length of the Fe increases after the second threshold and it is hypothesized that the increase is due to the momentum distribution of the second conduction band minimum at the interface.

II. EXPERIMENT

Two types of Schottky diodes were fabricated using commercially available phosphorous-doped Si (001) wafers ($\rho = 120\ \Omega$ cm, $N_a = 3.6 \times 10^{13}$) diced into 5 mm × 5 mm pieces. Prior to deposition an Ohmic contact was made to the backside of these wafers by melting indium after scratching the surface with a diamond scriber. The native oxide was removed with a 49% hydrofluoric acid and de-ionized water solution immediately before being introduced into a Varion 980 electron beam evaporator which was then evacuated to a minimum base pressure of 3×10^{-6} mbar. Fe was evaporated from a graphite crucible for the first type of sample and a boron nitride crucible for the second type. Film thickness was monitored with a quartz microbalance. An additional layer of 13 nm of Au was deposited on top of the Fe films to prevent oxidation when mounting the samples *ex situ* to the BEEM sample holder. The samples were mounted to the sample holder using silver paste to the indium contact while a BeCu clip served as the front side contact. The silver paste allowed the indium on the sample to be mechanically and

 ©2006 The American Physical Society

electrically fixed to the indium on the sample holder without any heating of the sample after the deposition. Once prepared, these samples were introduced into a UHV chamber with a base pressure of 4×10^{-11} mbar and loaded onto the STM stage that had been cooled to 80 K for all BEEM measurements.

Rutherford backscattering spectrometry (RBS) was performed on the samples to measure their thickness. In addition, Auger electron spectroscopy (AES) sputter depth profiling was performed using a Perkin-Elmer PHI 600 scanning Auger microprobe with a base pressure of 7×10^{-9} mbar to measure the Fe to C atomic ratio in the samples. Compositional sputter depth profiling was accomplished by focusing a 2-keV argon ion beam on the surface while recording the elemental peaks for the film species and silicon as a function of sputter time. These data were then converted to atomic composition versus depth by applying the most appropriate relative sensitivity factors (derived empirically from pure standards) and the sputter rate for SiO_2. These measurements determined that the average peak ratio of Fe to C was 81:19 (±5%) across all samples made with the graphite crucible referred to as $Fe_{81}C_{19}$. Approximately 4% C was found in the samples made from the boron nitride crucibles referred to as Fe. The AES depth profile and RBS measurements did not show the presence of a silicide in either type of sample. However, some intermixing is likely to occur, eventually degrading the diode, but at 80 K the samples were found to be rectifying for up to 3 days, which was enough time to complete the measurements.

A modified low-temperature (4–300 K) UHV STM system (Omicron) was utilized to perform the BEEM measurements and has been described elsewhere.[14] The STM stage was in contact with a cryostat which was cooled with liquid nitrogen, resulting in a tip and sample temperature of approximately 80 K as measured by a Si diode mounted on the imaging stage. BEEM spectroscopy was performed using both W ⟨111⟩ tips for the $Fe_{81}C_{19}$ samples and Au tips for the Fe samples. The W ⟨111⟩ tips were manufactured from single-crystal, ⟨111⟩-oriented tungsten wire that was electrochemically etched to a sharp point in a 5-mol potassium hydroxide solution and electron beam heated *in situ* to remove any oxide. The Au tips were manufactured by cutting 10-mil diameter wire at a sharp angle. For each sample spectroscopy was performed at a minimum of 100 locations over an area of about 5 μm$\times$5 μm. The spectra were averaged together in order to reduce the effects of surface roughness on the BEEM current. STM images were used to calculate this rms roughness which was determined to be approximately 1 nm.

III. RESULTS

The BEEM current obtained from Fe and $Fe_{81}C_{19}$ samples remains nonexistent until the tip bias supersedes a threshold voltage at which point there is a rapid increase as seen in Fig. 1. The Schottky barrier of the $Fe_{81}C_{19}$ samples was found to be 0.68±0.02 eV by least-squares fitting of the data (open squares) to the modified (n=5/2) Bell-Kaiser (BK) model as shown by the dotted line in Fig. 1.[15] A dual threshold in the onset of the BEEM current was observed in the Fe/Si (001) samples (solid squares) with a Schottky height of 0.70±0.02 eV and a second threshold of 1.29±0.04 eV. Least-squares fits to the modified BK model for both a double- and single-threshold voltage were performed and shown as solid and dashed lines in Fig. 1, respectively.

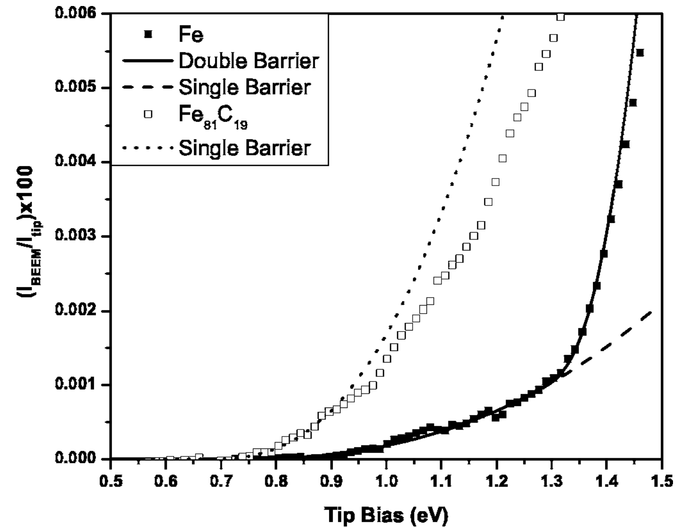

FIG. 1. Open squares: BEEM spectra from a 13-nm Au/13.8 nm $Fe_{81}C_{19}$/Si (001) sample. The dotted line indicates the fit to the modified Bell-Kaiser (BK) model with a Schottky barrier of 0.68±0.02 eV. Solid squares: BEEM spectra from a 13-nm Au/15.8 nm Fe/Si (001) sample. The solid line represents a fit to a double-threshold BK model with a Schottky height of 0.70±0.02 eV and a second threshold at 1.29±0.04 eV. The dashed line is a fit to the single-threshold BK model.

The logarithm of the percent transmission of the ballistic electrons, $I_{BEEM}/I_{tip}\times100$, acquired at a tip bias of 1.25 eV and 1.5 eV for all samples is plotted versus metal film thickness in Figs. 2(a) and 2(b), respectively. The line through each set of data points is the least-squares fit to

$$\frac{I_{BEEM}}{I_{tip}} = C(E,T)\exp[-d/\lambda(E,T)], \quad (1)$$

where I_{BEEM} and I_{tip} are the respective currents measured, $C(E,T)$ is a proportionality constant that accounts for scattering due to interfaces or within the semiconductor, d is the thickness of the metal, $\lambda(E,T)$ is the hot electron attenuation length, E is the electron energy, and T is the temperature. From this fit attenuation lengths of 3.0±0.9 nm and 3.5±1.0 nm were found at 1.25 eV while at 1.5 eV they were found to be 8.7±0.8 nm and 2.5±0.6 nm for the Fe and $Fe_{81}C_{19}$ samples, respectively.

The attenuation length was measured for tip biases ranging from 1.0 eV to 1.5 eV for both types of samples and displayed in Fig. 3. For the Fe sample, the attenuation length was found to decrease with increasing bias until it reaches 1.25 eV, after which the attenuation length begins to increase. The attenuation length in the $Fe_{81}C_{19}$ decreases with tip bias throughout the entire range.

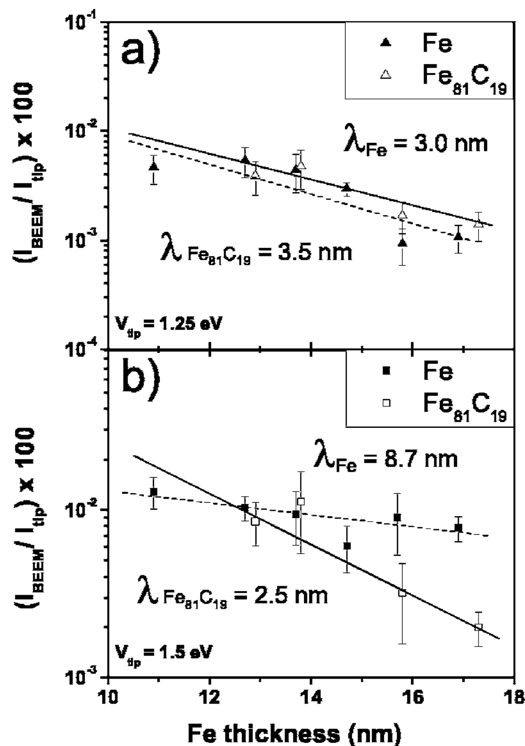

FIG. 2. Semilogarithmic plot of the percent transmission of the ballistic electrons for the $Fe_{81}C_{19}$ and Fe samples. The solid ($Fe_{81}C_{19}$) and dashed lines (Fe) represent the linear least squares fit giving attenuation lengths. (a) At a tip bias of 1.25 eV the attenuation lengths were found to be 3.0 ± 0.9 nm and 3.5 ± 1.0 nm while (b) at a tip bias of 1.5 eV they were found to be 8.7 ± 0.8 nm and 2.5 ± 0.6 nm for the Fe and $Fe_{81}C_{19}$ samples, respectively.

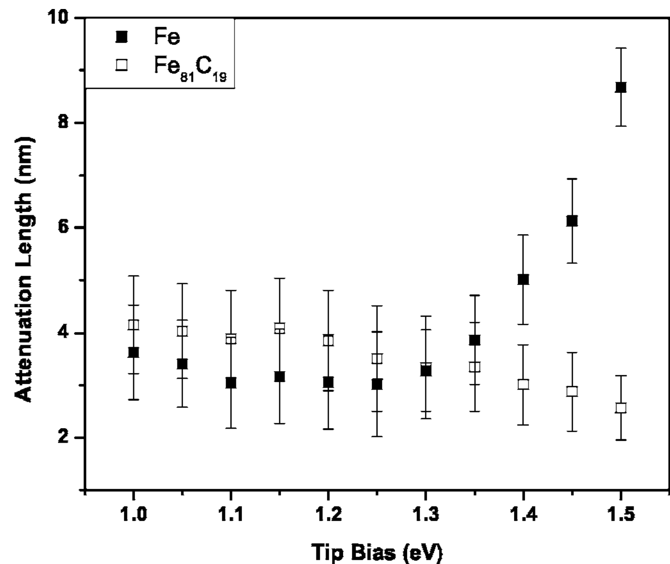

FIG. 3. Hot attenuation length as a function of tip bias for the $Fe_{81}C_{19}$ and Fe samples.

IV. DISCUSSION

Interestingly, the BEEM spectra from the Fe/Si (001) samples show the existence of two threshold voltages, while the $Fe_{81}C_{19}$/Si (001) sample displayed only a single-threshold voltage. The existence of more than one threshold voltage in a BEEM spectrum arises from electrons accessing additional conduction bands in the semiconductor at higher energies and has been observed for Au/GaAs (001) and Pd/SiC interfaces.[16,17] The existence of multiple-threshold voltages for a metal on Si (001) is not expected since Si (001) has only a single on-axis CBM, which has been confirmed using BEEM for Au on Si.[18] However, transition-metal–silicon interfaces are necessarily more complex than interfaces with ideal metals such as Au and may form entirely new interface band structures with multiple CBM's. For example, multiple thresholds have been recently observed for the MnSi/Si (001) interface and attributed to a complex interface band structure arising from the bonding at the Mn-Si interface.[10] In addition, interface band structures and resulting BEEM spectra have been theoretically predicted to be sensitive to the interface structure of the $NiSi_2$/Si (111) interface.[7–9] The observance of the double threshold in the Fe/Si (001) sample indicates that this interface has an additional CBM approximately 0.6 eV above the first minimum. In addition, the observation of only a single threshold when C in introduced into the film shows the interface band structures sensitivity to chemical composition. This information may prove useful to future theoretical studies of these types of interfaces.

The undershooting of the data from the BK model of the $Fe_{81}C_{19}$ samples about 0.2 eV above the Schottky height indicates that more scattering is occurring than in a metal such as Au where fits up to about 0.8 eV above the Schottky barrier are routinely obtained.[2] The Fe film has a better fit for the initial threshold voltage, but shows an undershooting of about 0.1 eV above the second threshold. The difference in the fit qualities between these two films may arise from differences in the interface scattering properties.

The attenuation length in Fe at 1.25 eV is approximately equal to that found in the $Fe_{81}C_{19}$ sample as displayed in Fig. 2(a). However, at 1.5 eV the measured Fe attenuation length is 3.5 times greater than in the $Fe_{81}C_{19}$ sample as displayed in Fig. 2(b). This indicates that at lower tip biases the additional carbon has little effect on electron transport in Fe for these film thicknesses. The large error bars on these plots are attributed to the large rms roughness seen in the STM images. To better understand the large difference in the attenuation lengths at higher tip biases it is best to first look at the attenuation lengths as a function of tip bias.

A decrease in the attenuation length with tip bias is observed in both samples and displayed in Fig. 3. This decrease was persistent in the $Fe_{81}C_{19}$ films through the entire energy range and persistent only between 1.0 and 1.25 eV in the Fe films. It has been determined that in Au films elastic defect scattering was the dominant scattering mechanism at these energy ranges which does not display an energy dependance.[19] However, an energy-dependent decrease was observed in $CoSi_2$ films for electron energies up to 6 eV.[20] This decrease was attributed to electron-electron scattering in the $CoSi_2$ film. Inelastic electron-electron scattering arises from the electrons interaction with the plasma energy of an electron gas in a metal. The attenuation length is proportional to $(E+E_f)/E^2$, where E_f is the Fermi energy.[21] Using this

formula, over the energy range of 1.0–1.2 eV the attenuation length of electron-electron scattering would be expected to decrease ~29% in the Fe film. The data in Fig. 3 show a decrease of ~16% for Fe and a decrease of ~17% for the $Fe_{81}C_{19}$ sample, indicating that the addition of C does not significantly affect the rate of electron-electron scattering. The difference between the experimental and theoretical energy decrease may be attributed to the nonideal Fermi surface of these transition metals.

Most striking is the sudden increase in the attenuation length in the Fe films that occurs above the second threshold. This increase means that the electron-electron scattering observed at lower energies is being overcome due to a change in the ballistic electron transport properties of the diode at these higher energies. The observation that this crossover occurs at approximately the same value as the second threshold suggests that this increase is related to the interface band structure even though the attenuation length is a property of the metal. For example, if the second threshold has a larger amount of available parallel-momentum states with greater parallel momentum when compared to the energy band associated with the Schottky barrier, then more electrons would be able to access these states as electrons are elastically scattered in the thicker films. As the tip bias is increased through the second threshold, electrons with greater parallel momentum will be allowed into the semiconductor. This effect will make the BEEM current less sensitive to thickness-dependent scattering in the metal at tip biases greater than the second threshold, giving the illusion that the attenuation length is increasing. This finding demonstrates the power of BEEM to probe the interface band structure between metals and semiconductors. However, this explanation has significant consequences for attenuation lengths measured using BEEM. As a result, more thickness-dependent BEEM studies are needed on other multiple-threshold systems to confirm this speculation.

Previous BEEM studies of Fe thin films between 0.2 and 2 nm have yielded attenuation lengths of 0.5 nm for Fe thicknesses at room temperature, nearly an order of magnitude less than what is reported here at 80 K.[12] Temperature alone cannot explain this difference as previous studies on Au showed only a 10% decrease in attenuation length between room temperature and 77 K.[19] This discrepancy can be explained due to the different range in thicknesses used in both studies, 0.2–2 nm and 11–17 nm, respectively. It has been shown that the attenuation length can become much shorter for thinner films due to the electrons making multiple attempts to cross the interface due to multiple reflections at the metal/vacuum and metal/semicondutor interfaces.[22] This increases the amount of BEEM current that is measured for thinner films which effectively shortens the measured attenuation length. As the metal thickness is increased, the opportunity for an electron to make multiple attempts to cross the metal-semiconductor interface decreases rapidly, increasing the measured attenuation length.

V. CONCLUSIONS

This study shows that BEEM is a powerful tool for studying the hot electron transport properties of ferromagnetic metal films as well as their interface band structure with semiconductors. It was found that the carbon did not significantly alter the Schottky height or attenuation length for energies less that 1.25 eV. However, the interface of the Fe/Si (001) showed the existence of an additional CBM, while the introduction of carbon into the Fe suppressed the additional threshold. The energetic dependence of the attenuation length for the Fe film suggests that the interface band structure may have an effect on attenuation lengths measured using BEEM.

ACKNOWLEDGMENTS

This work was supported by National Science Foundation Grant No. CAREER-DMR-0349108 and the MARCO Interconnect Focus Center.

[1] J. P. Park and P. A. Crowell, Phys. Rev. Lett. **95**, 167201 (2005).
[2] W. J. Kaiser and L. D. Bell, Phys. Rev. Lett. **60**, 1406 (1988).
[3] L. D. Bell and W. J. Kaiser, Annu. Rev. Mater. Sci. **26**, 189 (1996).
[4] M. Prietsch, Phys. Rep. **253**, 163 (1995).
[5] H. Sirringhaus, E. Y. Lee, and H. von Känel, Phys. Rev. Lett. **74**, 3999 (1995).
[6] M. D. Stiles and D. R. Hamann, J. Vac. Sci. Technol. B **9**, 2394 (1991).
[7] M. D. Stiles and D. R. Hamann, Phys. Rev. Lett. **66**, 3179 (1991).
[8] M. D. Stiles and D. R. Hamann, Phys. Rev. B **38**, 2021 (1988).
[9] H. D. Hallen, A. Fernandez, T. Huang, J. Silcox, and R. A. Buhrman, Phys. Rev. B **46**, 7256 (1992).
[10] A. Stollenwerk, M. Krause, R. Moore, and V. P. LaBella, J. Vac. Sci. Technol. A **24**, 1610 (2006).
[11] R. P. Lu, B. A. Morgan, K. L. Kavanagh, C. J. Powell, P. J. Chen, F. G. Serpa, and W. F. Egelhoff, Jr., J. Vac. Sci. Technol. B **18**, 2047 (2000).
[12] R. P. Lu, B. A. Morgan, K. L. Kavanagh, C. J. Powell, P. J. Chen, F. G. Serpa, and W. F. Egelhoff, Jr., J. Appl. Phys. **87**, 5164 (2000).
[13] A. J. Stollenwerk, M. R. Krause, D. H. Idell, R. Moore, and V. P. LaBella, J. Vac. Sci. Technol. B **24**, 2009 (2006).
[14] M. Krause, A. Stollenwerk, C. Awo-Affouda, B. Maclean, and V. P. LaBella, J. Vac. Sci. Technol. B **23**, 1684 (2005).
[15] M. Prietsch and R. Ludeke, Phys. Rev. Lett. **66**, 2511 (1991).
[16] L. D. Bell and W. J. Kaiser, Phys. Rev. Lett. **61**, 2368 (1988).
[17] B. Kaczer, H. J. Im, J. P. Pelz, J. Chen, and W. J. Choyke, Phys. Rev. B **57**, 4027 (1998).
[18] N. W. Ashcroft and N. D. Mermin, *Solid State Physics* (Saunders College, New York, 1976).
[19] C. A. Ventrice, Jr., V. P. LaBella, G. Ramaswamy, H. P. Yu, and L. J. Schowalter, Phys. Rev. B **53**, 3952 (1996).
[20] E. Y. Lee, H. Sirringhaus, U. Kafader, and H. von Känel, Phys. Rev. B **52**, 1816 (1995).
[21] J. J. Quinn, Phys. Rev. **126**, 1453 (1962).
[22] L. D. Bell, J. Vac. Sci. Technol. A **15**, 1358 (1997).